

Fundamental accuracy-resolution trade-off for timekeeping devices

Florian Meier,^{1,2,*} Emanuel Schwarzhans,^{1,†} Paul Erker,^{1,3,‡} and Marcus Huber^{1,3,§}

¹Vienna Center for Quantum Science and Technology,

Atominstytut, Technische Universität Wien, 1020 Vienna, Austria

²Institute for Theoretical Physics, ETH Zurich, 8093 Zürich, Switzerland

³Institute for Quantum Optics and Quantum Information,
Austrian Academy of Sciences, 1090 Vienna, Austria

(Dated: February 8, 2023)

From a thermodynamic point of view, all clocks are driven by irreversible processes. Additionally, one can use oscillatory systems to temporally modulate the thermodynamic flux towards equilibrium. Focusing on the most elementary thermalization events, this modulation can be thought of as a temporal probability concentration for these events. There are two fundamental factors limiting the performance of clocks: On the one level, the inevitable drifts of the oscillatory system, which are addressed by finding stable atomic or nuclear transitions that lead to astounding precision of today's clocks. On the other level, there is the intrinsically stochastic nature of the irreversible events upon which the clock's operation is based. This becomes relevant when seeking to maximize a clock's resolution at high accuracy, which is ultimately limited by the number of such stochastic events per reference time unit. We address this essential trade-off between clock accuracy and resolution, proving a universal bound for all clocks whose elementary thermalization events are memoryless.

Clocks dominate our daily lives unlike any other technology – from ordinary things like catching the train in the morning to locating ourselves using the GPS – they are involved everywhere and have been omnipresent since the dawn of human civilization. From the sundials of Mayan times to the UTC standard of today, over the centuries, physics provided the theoretical and experimental foundation to develop accurate and stable clocks. In the 50s, this development has taken a sharp turn with the invention of atomic clocks [1]. Year by year, these clocks have been improving their accuracy. Running a state-of-the-art optical clock is so accurate that it accumulates less than a hundred milliseconds of error over the lifespan of the sun [2–4]. These advancements beg for the question whether there are any physical principles that constrain the performance of a clock. Driven by this open problem, quantum clocks are emerging into an independent field of research, unifying approaches from quantum information theory [5–8] and quantum thermodynamics [9–13]. Recent experiments showcase today's technology is capable of exploring these ultimate limits of timekeeping [14–16].

This letter explores fundamental limitations of clocks coming from thermodynamics, because clocks, like all other physical systems, are subject to thermodynamical laws [11]. Even worse, they very much rely on the increase of entropy originating in the second law of thermodynamics. This implies that (1) clocks are witnesses of the macroscopic breaking of time-reversal symmetry because they tick forwards in time. (2) Thus, they must be driven by irreversible processes that drain out-of-equilibrium resources to output temporal information. These processes, though, are thermodynamic, therefore inherently stochastic and never perfectly predictable. (3) We conclude, even an idealized clock could never be perfect simply due to the fact that the clock itself is fundamentally driven by stochastic processes.

We look at clocks that use this flow by counting elementary thermalization events to define *ticks*. Instructive examples of such a process could range from grains of sand that pass through an hourglass to the photons that are reflected from a pendulum to ascertain its position. Even modern atomic clocks ultimately rely on a macroscopic number of photons to read out the laser frequency (which is stabilized by feedback from atomic transitions). In all these cases, the underlying thermalization processes are stochastic and have some intrinsic rate Γ . The time passing between two events, relative to assumed smooth parameter time, is probabilistic and described by a probability density function. We refer to its average as μ and its uncertainty as σ . We define the *resolution* ν of the clock to be the inverse average time between two ticks $\nu = 1/\mu$, and the *accuracy* N as the average number of times the clock ticks until it is off by one tick. For a sequence of independent and identically distributed ticks, the accuracy equals the signal-to-noise ratio $N = \mu^2/\sigma^2$. A clock usually modulates the temporal distribution of when the thermalization events occur as to improve its accuracy. For most practical clocks, the stability of this temporal modulation (for instance the laser frequency in atomic clocks) is the limiting factor to the accuracy. We show that even if this temporal modulation is perfectly stable, the stochastic process underlying the tick generation limits the accuracy at given resolution. In other words, the need to irreversibly generate a signal bounds the clock's performance even if it uses an eternally stable frequency reference.

Theorem (Accuracy-resolution trade-off). *Clocks with elementary ticking events generated by a memoryless stochastic process at rate Γ obey the trade-off relation*

$$N \leq \frac{\Gamma^2}{\nu^2}. \quad (1)$$

This trade-off complements other established results in the field considering restrictions imposed on the clock through entropy production [9, 17] or Hilbertspace dimension [18, 19].

Temporal probability concentration. The most primitive clock consists of two out-of-equilibrium thermal reservoirs in contact with each other. Counting the individual stochastic thermalization events as ticks can serve as a way to measure time, we call this the *thermal reference clock*. Sufficiently large reservoirs are memoryless, therefore, these events become exponentially distributed [20–22]. The coupling of the two baths defines a characteristic thermalization rate Γ . For an exponential distribution the standard deviation equals the average, which leads to $\mu = \sigma = \Gamma^{-1}$. Consequently, such a clock has unit accuracy $N = 1$ and only by averaging over many of these ticks are we able to achieve higher accuracy, but at the expense of resolution. Averaging over M independent and identically distributed (i.i.d.) such events increases the variance and mean of the tick time M -fold, leading to a resolution $\nu \propto 1/M$ and accuracy $N \propto M$. This gives an inverse proportional accuracy-resolution scaling

$$N = \frac{\Gamma}{\nu}, \quad (2)$$

quadratically smaller than the upper bound in eq. (1). Upon closer inspection, we find a thermodynamic cost associated to this increase in accuracy: instead of having a single irreversible event producing a tick, now M irreversible events are required.

A natural question to ask is whether it is possible to increase the accuracy beyond what is achievable through averaging in eq. (2), while still using the same underlying stochastic tick generating process. The answer lies in the observation that all ticking clocks known to us use a combination of two processes to tell time:

- (a) irreversible processes that generate ticks, and
- (b) a filter process, *temporal probability concentration*, which modulates the probability of the irreversible ticking events to occur.

By means of temporal probability concentration (TPC), a (sensible) clock centers the probability distribution of the stochastic events with a periodic process such that the ticks occur closely around well-defined instants in time. A thermodynamically optimal strategy would be to sample the periodic process with a single equilibration event per cycle [9, 10, 23], as we show in Figure 1. One microscopic example of such a clock could be a leaky cavity where an autonomous process induces Rabi oscillations. These oscillations temporally concentrate the population of the cavity that can leak out and generate a tick. Many macroscopically sized clocks, be it pendulums or atomic clocks, operate in an oversampling regime, where multiple irreversible events occur per TPC cycle (see Figure 2). In this regime, the thermodynamic cost of a clockwork often becomes obscure, as both the dissipation due to the macroscopic number of irreversible

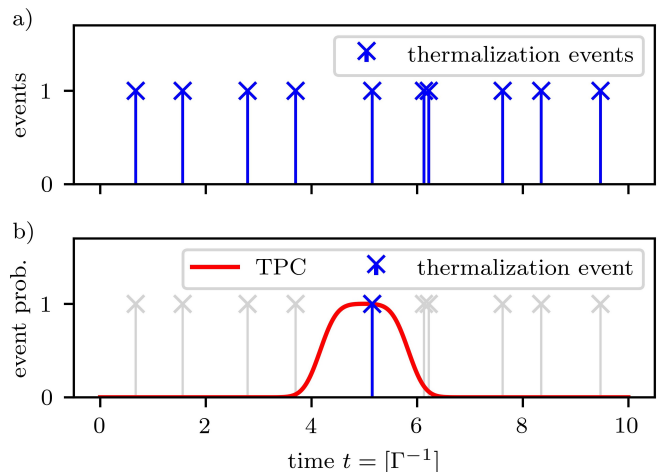


FIG. 1. The two plots qualitatively show the ticking behavior of two clocks with respect to parameter time t (horizontal axis). The ticks of such a clock are generated by individual thermalization events at rate Γ (vertical stripes with cross on top). Figure a) sketches a generic example, where these thermalization events are Poisson distributed. In b), temporal probability concentration is shown, another process through which the probability of an thermalization event can be suppressed at times (shown by the hat-shaped curve). As a result, the probability density for a tick can be concentrated around a desired average value, here $5 \Gamma^{-1}$, with the tick time uncertainty of order Γ^{-1} bounded by the width of the TPC window.

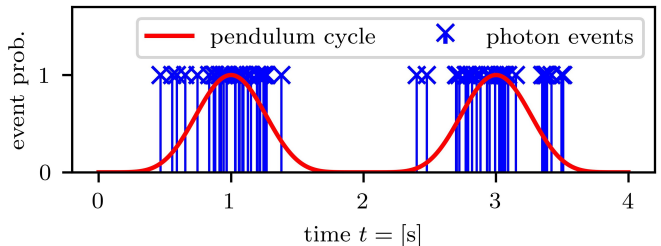


FIG. 2. We sketch the oversampling regime of an exemplary clock: a pendulum in a weakly lit environment. The two sources of entropy production for this clock are first of all the friction within the clockwork itself and secondly, the matter light interaction necessary to track the position of the pendulum. The plot shows the elementary ticking events of this clock as a function of time, i.e., the photons reflected off the pendulum when it is close to its maximum deflection. In the oversampling regime, the average time between two such ticks is much shorter than that of the period of the TPC (continuous line), which in the case of this pendulum is 2s. Due to technical limitations, one does not count photons, but rather the TPC cycles through the averaged light intensity.

events and the TPC have to be accounted for. Atomic clocks, for example, do not count photons as a way to tell time, rather they use the oversampled coherent oscillations of a maser tuned some stable reference atomic transition to estimate the TPC frequency. The time-scale Γ of the fundamental ticking events appearing in eq. (1)

is therefore not the limiting factor to the accuracy of atomic clocks, the stability of the coherent oscillation of the electromagnetic field is, i.e., the TPC stability. In atomic clocks, accuracy is examined using Allan Variance which captures the stability of the TPC oscillation over many different time-scales [24–26]. Quantum projection noise, thermal noise but also natural drifts in the experimental setup are what affect the stability of atomic clocks [27, 28].

So far, we have established that every clock is subject to irreversible processes and that through TPC, they can increase their accuracy. In the following, we introduce a mathematical model to describe clocks on a quantum scale and where the two contributions (a) irreversible ticks and (b) temporal probability concentrations have an explicit representation in the equations of motion. Eventually, this framework allows us to formulate the fundamental trade-off between the accuracy and resolution of clocks, dictated by thermodynamics.

Model. Quantum clocks [8–10, 18, 23] only weakly coupled to a memoryless environment (sufficiently large thermal baths are one such environment) can be described by a Lindblad master-equation [29]. If we are again talking about ticking clocks, their state can be Fourier-decomposed by introducing a free counting field χ [30],

$$\rho_C(t, \chi) = \sum_n \rho_C^{(n)}(t) e^{in\chi}. \quad (3)$$

Each non-normalized density matrix $\rho^{(n)}(t)$ can be thought of as the system’s state conditioned on n ticks having already occurred. Clocks that reset to the same state after they tick regardless of how many times they have ticked before give rise to an i.i.d. sequence of ticks. This class of clocks is particularly interesting, as their ticking statistics are entirely determined by the first tick, and it is sufficient to consider the evolution of the non-normalized state $\rho^{(0)}$. In a setting where the interactions with the environment are memoryless, the (first) ticks are generated by linear jump operators J_j . Aside from this, the clock is subject to a general open quantum system’s evolution with Lindblad operator \mathcal{L}_0 , which leads us to write the equations of motion of the clock’s state (where no tick has yet occurred) as

$$\dot{\rho}_C^{(0)}(t) = \mathcal{L}_0[\rho_C^{(0)}(t)] - \frac{1}{2} \sum_j \left\{ J_j^\dagger J_j, \rho_C^{(0)}(t) \right\}. \quad (4)$$

Ticking statistics. The right-most term of eq. (4) is responsible for the drain of population from the no-tick state $\rho_C^{(0)}$ to the state of the clock that has ticked once $\rho_C^{(1)}$. If we take the random variable T to describe the time of the first tick, the cumulative probability $P[t \leq T]$ that no tick has occurred up to time t equals the trace $P[t \leq T] = \text{tr} \rho_C^{(0)}$. There is an equivalent way of writing the cumulative tick probability by looking at the clock’s state conditioned on not having decayed $\rho_C^{\text{no tick}} =$

$\rho_C^{(0)} / \text{tr} \rho_C^{(0)}$. Using this state, the tick probability can alternatively be written as the exponential

$$P[t \leq T] = \exp\left(-\int_0^t dt' \text{tr}(V \rho_C^{\text{no tick}}(t'))\right), \quad (5)$$

where $V = \sum_j J_j^\dagger J_j$ is the positive operator generating the clock’s ticks [31]. This formulation faithfully represents the two processes that run a clock. The irreversible tick generating process (a) is represented by the underlying exponential and the operator V , whereas the TPC (b) lies in the time-evolution of the clock’s no-tick state, i.e., $\rho_C^{\text{no tick}}(t')$. In this sense, one may attempt to separate (a) and (b) into two independent processes, as in [10]; however the back-action of the tick channel always affects the clock evolution which is an inherent feature of clocks that operate on a quantum scale.

The master-equation description of quantum ticking clocks allows us to formalize the statement made in the accuracy-resolution trade-off theorem. The tick channel is governed by the positive operator V , whose spectral decomposition reveals the time-scales involved in the decay. We define the rate Γ as the fastest one of them,

$$\Gamma := \|V\|_{\max} = \max_{\rho \in \mathcal{S}(\mathcal{H}_C)} \text{tr} V \rho, \quad (6)$$

where the maximum is taken over all possible clock states $\rho \in \mathcal{S}(\mathcal{H}_C)$. This is consistent with the special case of exponential decay (as used in [9, 17]) with rate Γ , since there, the tick generator is given by a single jump operator $J = \sqrt{\Gamma} |0\rangle\langle 1|$. If a clock is described by eq. (4) and produces its ticks by means of the generators J_j , then the accuracy is limited by the resolution, regardless of how well a possible clockwork in the background works. The resulting bound is eq. (1) from the accuracy-resolution trade-off theorem which we recall here for completeness,

$$N \leq \frac{\Gamma^2}{\nu^2},$$

and prove in the following.

Proof. The key observation is that no clock can on average tick faster than the decay process that mediates the ticks allows for. If the elementary ticks are generated by an ensemble of jump operators J_j , then the fastest such rate is given by Γ (see eq. (6)). A single such channel produces ticks that are exponentially distributed and as a consequence, we can reduce the generic form from eq. (5) to the special case of exponential decay, where the exponent reduces to $-\Gamma \int dt' p(t')$, and $p(t)$ is a measure of the clock’s state population that can decay. Regardless of how the TPC modulates $p(t)$, the variance σ^2 of the tick can never be smaller than Γ^2 , the variance of exponential decay. This is a manifestation of the fact that no clock can tick faster than it’s underlying decay process. Now that the variance σ^2 of the tick time distribution is bounded from above by Γ^2 , the main theorem follows. We refer the reader to Appendix A for a detailed account of the proof. \square

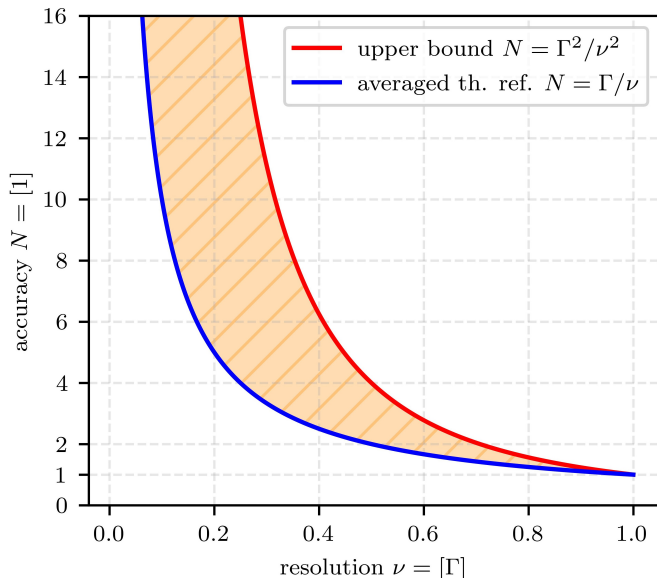


FIG. 3. In this figure, we plot the accuracy N on the vertical axis versus the resolution ν on the horizontal axis. The red curve highlights the upper bound for the accuracy $N = \Gamma^2/\nu^2$ given by the accuracy-resolution trade-off theorem. Below, we have the blue curve, indicating the accuracy and resolution that can be achieved by averaging the thermal reference clock with fundamental tick rate Γ . The green shaded area between the two curves contains all the accuracy-resolution couples that cannot be achieved by classically averaging a rate Γ stochastic process, but which are still allowed by the upper bound. How close one can get to the red curve with quantum clocks and whether classical clocks are constrained to be below the blue line are open questions.

In this letter, we have analyzed quantum timekeeping devices through a thermodynamic lens, where their tick generation can be decomposed into two processes, (a) a stochastic process which irreversibly produces the ticks and (b) temporal probability concentration (TPC) through a clockwork which controls when these elementary ticks occur. Then, we asserted that there is a fundamental trade-off between the clock’s accuracy and resolution (see trade-off theorem but also Figure 3), stating that the number of times a clock can tick until it goes wrong by one tick is universally bounded by the inverse of the clock’s resolution squared.

Atomic and optical clocks. These results have their validity in the regime where the number of fundamental thermalization events is directly used to define ticks. Macroscopic clocks such as atomic and optical ones work in a different regime, where the TPC is oversampled by irreversible events and ticks are defined not by event numbers directly, but rather those are used to estimate the oscillatory TPC process frequency. Atomic clocks working with a 10 dBm maser at the 21 cm line of hydrogen, for example, emit of the order of 10^{12} photons per period of the electromagnetic field oscillation. Given that the individual photons are exponentially distributed, a

(hypothetical) clock which counts the maser’s photons and averages over one second would achieve an accuracy of $N \sim 10^{21}$ compared to $N \sim 10^{13}$ that current-day commercial masers reach in terms of relative precision per second [32]. Accuracy restrictions coming from the elementary thermalization events are not the limiting factor when it comes to atomic clocks because of the macroscopic number of such events over which is averaged. The main sources of error are drifts due to changes in temperature, environmental electromagnetic fields and other experimental imperfections. Moreover, it is also important to keep in mind that atomic clocks do not generate independent and identically distributed ticks, as their real advantage comes from long-time stability achieved through feedback-control using an ultra-stable atomic transition which is not captured by the i.i.d. formalism herein presented.

Achievability. Good clocks excel by resolving time well while at the same time being highly accurate, i.e., maximizing both ν and N ; ideally, they do so at optimal thermodynamic costs far away from the oversampled regime and only with a single thermalization event per tick. As a foundational question, we may ask, does there exist an appropriate clock Lindblad operator \mathcal{L} , through which it is possible to saturate the bound $N = \Gamma^2/\nu^2$? And the answer is: No, at least not for finite systems. As it turns out, saturating this bound amounts to a time-dependent Lindblad-operator, which instantaneously rotates the clock state from a subspace of states where it can’t tick onto a state from which it decays at rate Γ (see details of the proof for the accuracy-resolution trade-off theorem in Appendix A). The TPC in this case would be ideal as it concentrates the decay event to the most narrow time-window possible, the one given by the underlying stochastic process, but quantum speed limits prohibit such an instantaneous state rotation for systems finite in energy and dimension [33–35]. A weaker question we can ask is whether at least the scaling $N = O(\Gamma^2/\nu^2)$ can be reached, and which resources are required for this. Without imposing any restriction on the clock’s Lindbladian aside from time-independence, there are quantum clocks which asymptotically reach the squared scaling of N for large dimensions of the clock Hilbert space [23]. To do so, they require highly coherent states, whose generation using only thermal resources is technically infinitely expensive from an entropic perspective [36] and the approximation with finite resources is an open problem. Of interest in the field of thermodynamics are the autonomous quantum clocks which only require thermal resources to run [9, 10, 12, 31], in particular no external control but also no coherence in the initial state. It is ongoing research, whether it is possible for such clocks to approach the optimal accuracy-resolution scaling.

Questions about fundamental precision limits are generally of great interest. The accuracy of clocks falls into this category and closely related problems have been examined in the field of (quantum) stochastic thermodynamics under the name of thermodynamic uncertainty

relations (TUR) [37–39] and kinematic uncertainty relations (KUR) [40–42]. Future work exploring connections between timekeeping and the TUR / KUR has to reveal whether a quantum thermodynamic advantage close to the optimal accuracy-resolution bound $N = \Gamma^2/\nu^2$ is in principle possible. Both superconducting circuits and optomechanical systems are promising platforms to test the achievability of the optimal accuracy-resolution relation while accounting for the resources and ensuring that they do not introduce a hidden clock through a backdoor.

We wish to acknowledge fruitful discussions and feedback from Ralph Silva, Nuriya Nurgalieva, Renato Renner, Maximilian Edward Lock and Jake Xuereb. F.M. and M.H. acknowledge the financial support from the Eu-

ropean Commission under the Horizon Europe project ASPECTS (Grant No. 101080167) and the ERC consolidator grant COCOQUEST (Grant No. 101043705). F.M. acknowledges the SEMP scholarship from Movetia for his research stay at Atominstytut, Technische Universität Wien. E.S. acknowledges the support from the Austrian Science Fund (FWF) through the START project Y879-N27, the ESQ Discovery grant “Emergence of physical laws: From mathematical foundations to applications in many body physics” and the ERC consolidator grant COCOQUEST (Grant No. 101043705). P.E. and M.H. further acknowledge funds from the FQXi (FQXi-IAF19-03-S2) within the project “Fueling quantum field machines with information”.

* florianmeier256@gmail.com

† e.schwarzahns@gmx.at

‡ paul.erker@tuwien.ac.at

§ marcus.huber@tuwien.ac.at

- [1] L. Essen and J. V. L. Parry, An Atomic Standard of Frequency and Time Interval: A Cæsium Resonator, *Nature* **176**, 280 (1955).
- [2] A. D. Ludlow, M. M. Boyd, J. Ye, E. Peik, and P. Schmidt, Optical atomic clocks, *Reviews of Modern Physics* **87**, 637 (2015).
- [3] F. Riehle, Towards a redefinition of the second based on optical atomic clocks, *Comptes Rendus Physique* **16**, 506 (2015), the measurement of time / La mesure du temps.
- [4] T. Bothwell, C. J. Kennedy, A. Aepli, D. Kedar, J. M. Robinson, E. Oelker, A. Staron, and J. Ye, Resolving the gravitational redshift across a millimetre-scale atomic sample, *Nature* **602**, 420 (2022).
- [5] S. Ranković, Y.-C. Liang, and R. Renner, *Quantum clocks and their synchronisation - the Alternate Ticks Game* (2015).
- [6] R. Renner and S. Stupar, eds., *Time in Physics* (Springer International Publishing, 2017).
- [7] S. Stupar, C. Klumpp, R. Renner, and N. Gisin, *Performance of stochastic clocks in the Alternate Ticks Game* (2018).
- [8] M. P. Woods, Autonomous Ticking Clocks from Axiomatic Principles, *Quantum* **5**, 381 (2021).
- [9] P. Erker, M. T. Mitchison, R. Silva, M. P. Woods, N. Brunner, and M. Huber, Autonomous Quantum Clocks: Does Thermodynamics Limit Our Ability to Measure Time?, *PRX* **7**, 031022 (2017).
- [10] E. Schwarzahns, M. P. E. Lock, P. Erker, N. Friis, and M. Huber, Autonomous Temporal Probability Concentration: Clockworks and the Second Law of Thermodynamics, *PRX* **11**, 011046 (2021).
- [11] G. J. Milburn, The thermodynamics of clocks, *Contemporary Physics* **61**, 69 (2020), <https://doi.org/10.1080/00107514.2020.1837471>.
- [12] S. K. Manikandan, *Autonomous quantum clocks using athermal resources* (2022).
- [13] D. Cilluffo, Statistical time-domain characterization of non-periodic optical clocks, *Quantum* **6**, 764 (2022).
- [14] A. N. Pearson, Y. Guryanova, P. Erker, E. A. Laird, G. A. D. Briggs, M. Huber, and N. Ares, Measuring the Thermodynamic Cost of Timekeeping, *Phys. Rev. X* **11**, 021029 (2021).
- [15] M. Berholts, R. Knut, R. Stefanuik, H. Wikmark, S. Saha, and J. Söderström, Quantum watch and its intrinsic proof of accuracy, *Phys. Rev. Res.* **4**, 043041 (2022).
- [16] X. He, P. Pakkiam, A. Gangat, G. Milburn, and A. Fedorov, *Measurement driven quantum clock implemented with a superconducting qubit* (2022).
- [17] A. C. Barato and U. Seifert, Cost and precision of brownian clocks, *Phys. Rev. X* **6**, 041053 (2016).
- [18] M. P. Woods, R. Silva, G. Pütz, S. Stupar, and R. Renner, Quantum Clocks are More Accurate Than Classical Ones, *PRXQUANTUM* **3**, 010319 (2022).
- [19] Y. Yang and R. Renner, *Ultimate limit on time signal generation* (2020).
- [20] R. S. Ingarden, A. Kossakowski, and M. Ohya, *Information Dynamics and Open Systems* (Springer Netherlands, 1997).
- [21] H.-P. Breuer and F. Petruccione, *The Theory of Open Quantum Systems* (Oxford University Press, 2007).
- [22] A. Klenke, *Probability Theory* (Springer International Publishing, 2020).
- [23] M. P. Woods, R. Silva, and J. Oppenheim, Autonomous Quantum Machines and Finite-Sized Clocks, *Annales Henri Poincaré* **20**, 125 (2019).
- [24] D. W. Allan, Statistics of atomic frequency standards, *Proceedings of the IEEE* **54**, 221 (1966).
- [25] D. W. Allan, N. Ashby, and C. C. Hodge, *The Science of Timekeeping Application Note 1289*, Hewlett Packard (1997), packard Application Note 1289.
- [26] W. Riley and D. Howe, *Handbook of Frequency Stability Analysis* (2008).
- [27] N. Shiga, M. Mizuno, K. Kido, P. Phoonthong, and K. Okada, Accelerating the averaging rate of atomic ensemble clock stability using atomic phase lock, *New Journal of Physics* **16**, 073029 (2014).
- [28] M. Schulte, C. Lisdat, P. O. Schmidt, U. Sterr, and K. Hammerer, Prospects and challenges for squeezing-enhanced optical atomic clocks, *Nature Communications* **11**, 5955 (2020).
- [29] G. Lindblad, On the generators of quantum dynamical semigroups, *Communications in Mathematical Physics* **48**, 119 (1976).

- [30] G. Schaller, *Open Quantum Systems Far from Equilibrium* (Springer International Publishing, 2014).
- [31] F. Meier, [Performance limits of decay clocks: Fundamental accuracy and resolution limits of quantum clocks with exponential ticking mechanism](#) (2022).
- [32] *MHM-2020 Active Hydrogen Maser*, Microchip Technology Inc. (2019), rev. 1.
- [33] L. Mandelstam, I. Tamm, and I. E. Tamm, The Uncertainty Relation Between Energy and Time in Non-relativistic Quantum Mechanics, in *Selected Papers*, edited by B. M. Bolotovskii, V. Y. Frenkel, and R. Peierls (Springer Berlin Heidelberg, Berlin, Heidelberg, 1991) pp. 115–123.
- [34] N. Margolus and L. B. Levitin, The maximum speed of dynamical evolution, *Physica D: Nonlinear Phenomena* **120**, 188 (1998), proceedings of the Fourth Workshop on Physics and Consumption.
- [35] S. Deffner and S. Campbell, Quantum speed limits: from heisenberg’s uncertainty principle to optimal quantum control, *Journal of Physics A: Mathematical and Theoretical* **50**, 453001 (2017).
- [36] P. Taranto, F. Bakhshinezhad, A. Bluhm, R. Silva, N. Friis, M. P. E. Lock, G. Vitagliano, F. C. Binder, T. Debarba, E. Schwarzthans, F. Clivaz, and M. Huber, [Landauer vs. Nernst: What is the True Cost of Cooling a Quantum System?](#) (2021), arXiv:2106.05151 [quant-ph].
- [37] A. C. Barato and U. Seifert, Thermodynamic Uncertainty Relation for Biomolecular Processes, *Phys. Rev. Lett.* **114**, 158101 (2015).
- [38] J. M. Horowitz and T. R. Gingrich, Thermodynamic uncertainty relations constrain non-equilibrium fluctuations, *Nature Physics* **16**, 15 (2020).
- [39] T. V. Vu and K. Saito, Thermodynamics of Precision in Markovian Open Quantum Dynamics, *Physical Review Letters* **128**, 140602 (2022).
- [40] I. D. Terlizzi and M. Baiesi, Kinetic uncertainty relation, *Journal of Physics A: Mathematical and Theoretical* **52**, 02LT03 (2018).
- [41] V. T. Vo, T. V. Vu, and Y. Hasegawa, Unified thermodynamic–kinetic uncertainty relation, *Journal of Physics A: Mathematical and Theoretical* **55**, 405004 (2022).
- [42] K. Prech, P. Johansson, E. Nyholm, G. T. Landi, C. Verdozzi, P. Samuelsson, and P. P. Potts, [Entanglement and thermo-kinetic uncertainty relations in coherent mesoscopic transport](#) (2022).

APPENDICES

Appendix A: Proof of the accuracy-resolution trade-off

Before we get started with the proof of the accuracy-resolution trade-off theorem (which is a generalization of the one shown in [31]), some preliminary notation has to be established. When it comes to the cumulative non-tick probability $P[t < T]$ as in eq. (5), the trace $\text{tr } V\rho_C(t)$ can be rewritten as

$$\text{tr}(V\rho_C(t)) = \Gamma p(t), \quad (\text{A1})$$

where $p : \mathbb{R}_{\geq 0} \rightarrow [0, 1]$ is a smooth function that takes values between 0 and 1. This comes from the fact that Γ is the maximum of the expression over all states ρ and the function can only take positive values because V is a positive operator. This expression puts us into the position, where we can write

$$P[t \leq T] = \exp\left(-\Gamma \int_0^t dt' p(t')\right), \quad (\text{A2})$$

which is formally the exact same expression that one would obtain in the case where the clock's elementary ticks are exponential decay. We will from now on refer to $p(t)$ as the *top-level population*. The remaining appendices are an adapted version of the proof of the accuracy-resolution theorem originally derived in [31].

1. The Heaviside- Θ population

Definition 1 (Heaviside populations). *The family of Heaviside populations comprises all the functions*

$$p^\Theta : \mathbb{R}_{\geq 0} \rightarrow [0, 1] \quad (\text{A3})$$

$$t \mapsto \Theta(t - t_0), \quad (\text{A4})$$

where $t_0 \geq 0$.

Properties of the Heaviside population. Such a top-level population is unphysical because of its discontinuity at time $t = t_0$. This is not an obstacle, though, as we only use the Heaviside population to prove an upper bound for the accuracy of a decay clock. No claim is made whether we can physically obtain the Heaviside population. The non-tick probability $P_\Theta[t \leq T]$ and tick probability density $p_{\text{tick}}^\Theta(t)$ associated to this population are given by (see eq. (A2))

$$P_\Theta[t \leq T] = \begin{cases} 1 & t \leq t_0 \\ e^{-\Gamma(t-t_0)} & t \geq t_0, \end{cases} \quad (\text{A5})$$

and

$$p_{\text{tick}}^\Theta(t) = \begin{cases} 0 & t \leq t_0 \\ \Gamma e^{-\Gamma(t-t_0)} & t \geq t_0. \end{cases} \quad (\text{A6})$$

See Figure 4 for a visualization of these functions. Using the analytic solution of the integral over an exponential, $\int_0^\infty dx e^{-ax} = 1/a$, we can calculate the accuracy and resolution for clocks working the Heaviside population.

Lemma 2. *The Heaviside population $p^\Theta(t) = \Theta(t - t_0)$ has an accuracy and resolution given by*

$$N = (1 + \Gamma t_0)^2, \text{ and } \nu = \frac{1}{t_0 + \frac{1}{\Gamma}}, \quad (\text{A7})$$

leading to an accuracy-resolution relation

$$N = \frac{\Gamma^2}{\nu^2}. \quad (\text{A8})$$

Before we prove Lemma 2, let us put the Heaviside population into perspective. Given the accuracy-resolution trade-off theorem the equality $N = \Gamma^2/\nu^2$ for clocks with Heaviside population tells us that this top-level population profile is ideal in the accuracy-resolution sense. This is no coincidence: a Heaviside population with offset at t_0 requires a clock in the background which perfectly knows t_0 . The population then describes a ladder conditioned on not having decayed, whose top-level is populated precisely at $t = t_0$, and stays there. This would require instantaneous external driving at $t = t_0$, i.e., a perfect background clock. The exponential decay channel coupled to the top-level then smears out the Heaviside profile of $p^\Theta(t)$ into an exponential decaying tick probability density $p_{\text{tick}}^\Theta(t)$ of width $1/\Gamma$, giving rise to the results of Lemma 2.

Proof. The average tick time is given by an integral over $tp_{\text{tick}}^\Theta(t)$ and splits into two parts

$$\mu = \int_0^\infty dt t p_{\text{tick}}^\Theta(t) = 0 + \int_{t_0}^\infty dt t e^{-\Gamma(t-t_0)} \quad (\text{A9})$$

$$= t_0 + \frac{1}{\Gamma}. \quad (\text{A10})$$

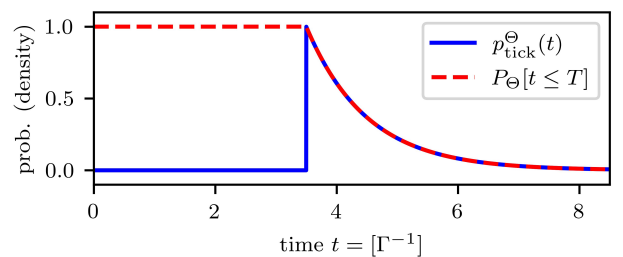


FIG. 4. This graph visualizes the ticking statistics for the Heaviside population. The solid line in the above figure visualizes the tick probability density, whereas the dashed line stands for the cumulative non-tick probability. The time axis scales in inverse units of the decay rate Γ and the population in the example is chosen such that on average the decay occurs at $\mu = 4.5 \Gamma$.

Thus, the resolution is given by $\nu = (t_0 + \frac{1}{\Gamma})^{-1}$. For the accuracy, which is defined as $N = (\mu/\sigma)^2$, we only need to calculate the variance σ^2 . The variance, however, is invariant under translations of the tick probability density and, thus, one can calculate the variance without loss of generality for $t_0 = 0$,

$$\sigma^2 = \int_0^\infty dt t^2 e^{-\Gamma t} - \mu^2 \quad (\text{A11})$$

$$= \frac{2}{\Gamma^2} - \frac{1}{\Gamma^2} = \frac{1}{\Gamma^2}. \quad (\text{A12})$$

Expressing the accuracy in terms of t_0 , we find $N = (1 + \Gamma t_0)^2$, that is, the accuracy increases with higher offset t_0 . There is a tradeoff, though: The greater t_0 , the lower the resolution. Eliminating the t_0 -dependency in the equations, we can establish an accuracy-resolution relation for the family of Heaviside populations given by $N = \Gamma^2/\nu^2$. \square

Analytic preliminaries. The tick probability density $p_{\text{tick}}(t)$ reveals how likely it is for a tick to happen during a given time interval. By the fundamental theorem of calculus, the cumulative non-tick probability $P[t \leq T]$ (whose negative derivative is $p_{\text{tick}}(t)$) contains the same information, and for proving the accuracy-resolution trade-off, the latter function turns out to be useful. Let us collect some general identities for the non-tick probability $P[t \leq T]$ which for some function $p(t)$ (be reminded, that the superscript *no tick* is suppressed) is given by

$$P[t \leq T] = e^{-\Gamma \int_0^t d\tau p(\tau)}. \quad (\text{A13})$$

There is a general constraint (Lemma 3) on how fast the non-tick probability decays. The fact that $p(t) \in [0, 1]$ ensures that $P[t \leq T]$ is monotonically decreasing (because the integral $\int_0^t d\tau p(\tau)$ is monotonically increasing) but does this not faster than exponentially.

Lemma 3. *For all $t > 0$ and $s > 0$, the cumulative non-tick probability satisfies the following inequalities:*

$$P[t \leq T]e^{-\Gamma s} \leq P[t + s \leq T] \leq P[t \leq T]. \quad (\text{A14})$$

Proof. This is a consequence of eq. (A13) and the fact that $0 \leq p(t) \leq 1$. \square

The cumulative non-tick probability can be used to calculate the moments of the probability density $p_{\text{tick}}(t)$ (see Definition 4 and Lemma 5) via the relation $p_{\text{tick}}(t) = -\dot{P}[t \leq T]$ and partial integration. It is important to note, that this discussion only makes sense for clocks that tick with certainty, i.e., $\lim_{t \rightarrow \infty} P[t \leq T] = 0$. This need not be true for all clocks, however, whenever we talk about a *tick probability density*, we implicitly assume that we have a properly normalized probability density in the probability theoretic sense [22].

Definition 4 (Moments). *For a given tick probability density $p_{\text{tick}}(t)$, define its k -th moment as*

$$t_k := \int_0^\infty dt t^k p_{\text{tick}}(t). \quad (\text{A15})$$

Lemma 5 (Tick probability moments). *The k -th moment of $p_{\text{tick}}(t)$ is related to $P[t \leq T]$ by the integral*

$$t_k = k \int_0^\infty dt t^{k-1} P[t \leq T]. \quad (\text{A16})$$

Proof. This is partial integration and for the boundary conditions, we use the assumption that $\lim_{t \rightarrow \infty} P[t \leq T] = 0$. \square

In particular, we can apply this result to $\mu = t_1$ and $\sigma = t_2 - \mu^2$, two expressions that are essential in Section A 2, where we prove the upper bound. The average tick time $\mu = t_1$ can be written as the area below the graph of $P[t \leq T]$,

$$\mu = t_1 = \int_0^\infty dt t p_{\text{tick}}(t) = \int_0^\infty dt P[t \leq T]. \quad (\text{A17})$$

The second moment t_2 , on the other hand, is related to the center of mass of the graph for $P[t \leq T]$, up to normalization,

$$t_2 = \int_0^\infty dt t^2 p_{\text{tick}}(t) = 2 \int_0^\infty dt t P[t \leq T]. \quad (\text{A18})$$

2. Proof construction

The introduction of the Heaviside population in Definition 1 together with the result in Lemma 2, that these populations achieved the (claimed) optimal accuracy resolution relation, leads us to the following approach in proving the inequality $N \leq \Gamma^2/\nu^2$: we try to show that all clocks are worse than the one with a Heaviside population, which has essentially a perfect background clock. In that sense, what we are showing is that no clock is better than the one that is already perfect. The only premise we have for the proof is that the clocks we consider eventually tick (i.e., $p_{\text{tick}}(t)$ is a valid probability density) and that their evolution is continuous,¹ we call this *well-behaved*. That being said, our strategy to prove the upper bound consists of the following three steps:

- (i) We show that for any well-behaved top-level population $p(t)$, there exists a Heaviside- Θ type top-level population with the same average tick time.

¹ This ensures we are doing a fair comparison, otherwise, we'd have to discuss how to compare clocks that possibly never tick to ones that always tick. We reserve that discussion for future work.

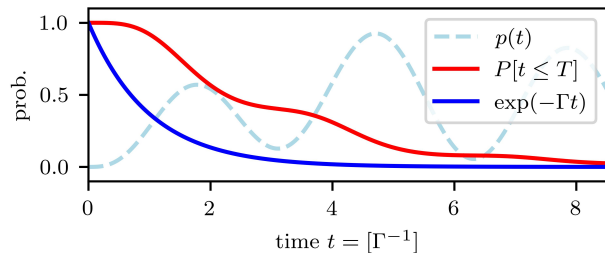


FIG. 5. The sketch shows the time-dependency of a generic top-level population $p(t)$ together with the associated cumulative non-tick probability $P[t \leq T]$ compared to the non-tick probability $e^{-\Gamma t}$ of the top-level population which is constantly 1. A top-level population smaller than unity leads to a slower decay of the non-tick probability, which is responsible for a lower bound on the average tick-time given by $1/\Gamma$.

- (ii) Then, we argue that the variance of the tick probability density coming from the Heaviside- Θ top-level population lower-bounds the variance coming from the generic population $p(t)$.
- (iii) We conclude that any well-behaved top-level population $p(t)$ must have an accuracy upper bounded by that of the Heaviside population and by using Lemma 2 on the properties of the Heaviside population, we have $N \leq \Gamma^2/\nu^2$. Once we are there, we have proven the accuracy-resolution trade-off theorem.

Step (i). Begin with a generic, but well behaved top-level population $p(t)$. Let μ be its average tick time and define $t_0 := \mu - 1/\Gamma$. The top-level population

$$p^\Theta(t) = \Theta(t - t_0) \quad (\text{A19})$$

has the same first moment $t_1 = \mu$ as the generic top-level population.² For the results from Lemma 2 to carry over, we need $t_0 > 0$. This is generally true as Lemma 6 guarantees. In fact, it tells us (see Figure 5) that the average tick time of any well-behaved top-level probability can not be smaller than $1/\Gamma$ and that the best resolution is achieved by the top-level population which is constantly one.

Lemma 6 (Resolution upper bound). *For any well-behaved top-level population $p : \mathbb{R}_{\geq 0} \rightarrow [0, 1]$, the induced resolution ν cannot be greater than Γ .*

Proof. Equivalently to the statement in the Lemma, we can prove that $\mu \geq 1/\Gamma$. For this matter, use eq. (A17), to estimate the average tick time

$$\mu = \int_0^\infty dt P[t \leq T] \geq \int_0^\infty dt e^{-\Gamma t} = 1/\Gamma. \quad (\text{A20})$$

² The average tick time is given by $\mu^\Theta = t_0 + 1/\Gamma$, with t_0 coming from the time translation of the Heaviside- Θ function and $1/\Gamma$ coming from the exponential decay.

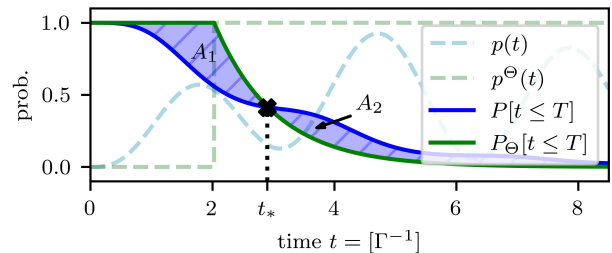


FIG. 6. The dashed lines show the top-level populations for the generic (blue) and the Heaviside case (green). The induced cumulative non-tick probabilities $P[t \leq T]$ and $P_\Theta[t \leq T]$ are drawn in the same color but as solid lines. The time t_* marks the unique crossing point of the two non-tick probabilities. On its right and left, the two areas A_1 and A_2 are defined by the difference between the two non-tick probabilities.

This concludes the proof. \square

Step (ii). If $p(t) = p^\Theta(t)$, there is nothing to be shown, because $p^\Theta(t)$ achieves the minimal tick time variance $\sigma^2 = 1/\Gamma^2$ (see eq. (A12)). Hence, we assume from now on $p(t) \neq p^\Theta(t)$ to avoid this pathological case. Proposition 8 in Appendix A3 further discusses, that there exists a unique $t_* > t_0 = \mu - 1/\Gamma$, such that $P[t_* \leq T] = e^{-\Gamma(t_* - t_0)}$ (see Figure 6). For all times $t < t_*$, the non-tick probability for the generic top-level population is smaller than that of the Heaviside population, i.e., $P[t \leq T] \leq P_\Theta[t \leq T]$. In the generic case, a tick before t_* is therefore more likely than for the Heaviside case. On the other hand, for all $t > t_*$, we have $P[t \leq T] \geq P_\Theta[t \leq T]$. That is, in the generic case, it is also more likely that after t_* the tick did not happen. Formally, the variance of the tick signal is bigger for a generic population than for the Heaviside one (Proposition 7).

Proposition 7. *For any well-behaved top-level population $p : \mathbb{R}_{\geq 0} \rightarrow [0, 1]$, the variance of the tick probability density $p_{\text{tick}}(t)$ is lower-bounded by that of $p_{\text{tick}}^\Theta(t)$, the tick probability density coming from the Heaviside top-level population $p^\Theta(t)$ defined in eq. (A19).*

Proof. By construction both $p_{\text{tick}}(t)$ and $p_{\text{tick}}^\Theta(t)$ have the same average tick time μ . Because the variance of the tick time is given by the difference $\sigma^2 = t_2 - \mu^2$, the following two statements are equivalent,

$$\sigma^2 \geq \sigma_\Theta^2 \Leftrightarrow t_2 \geq t_2^\Theta. \quad (\text{A21})$$

The second moments on the right-hand side can be calculated as the center of mass of the respective non-tick probabilities $P[t \leq T]$ and $P_\Theta[t \leq T]$ (up to constant prefactors, see also eq. (A18)). Therefore, the question we have to answer is, whether the graph of $P[t \leq T]$ has a center of mass at larger values of t than that of $P_\Theta[t \leq T]$? The two areas A_1 and A_2 in Figure 6 are equal and they correspond to the difference in the area

below the graphs of $P[t \leq T]$ and $P_\Theta[t \leq T]$. The graph of $P[t \leq T]$ has less ‘mass’ (i.e., area) on the interval $0 \geq t \geq t_*$ than $P_\Theta[t \leq T]$. For $t_* \geq t \geq \infty$, however, $P[t \leq T]$ has more ‘mass’, resulting in a center of mass further to the right for $P[t \leq T]$ than for $P_\Theta[t \leq T]$. Formally,

$$\frac{t_2}{2} = \int_0^\infty dt t P[t \leq T] \quad (\text{A22})$$

$$= \int_0^\infty dt t P_\Theta[t \leq T] + \int_0^\infty dt t \underbrace{(P[t \leq T] - P_\Theta[t \leq T])}_{:=\Delta P(t)} \quad (\text{A23})$$

$$\geq \int_0^\infty dt t P_\Theta[t \leq T] = \frac{t_2^\Theta}{2}, \quad (\text{A24})$$

where the inequality comes about because the integral over $\Delta P(t)$ is greater equal than zero,

$$\int_0^\infty dt t \Delta P(t) = \int_0^{t_*} dt t \Delta P(t) + \int_{t_*}^\infty dt t \Delta P(t) \quad (\text{A25})$$

$$\geq \int_0^{t_*} dt t_* \Delta P(t) + \int_{t_*}^\infty dt t_* \Delta P(t) = 0. \quad (\text{A26})$$

All in all, this shows that $t_2 \geq t_2^\Theta$, which, by the initial remark, proves the proposition. \square

Step (iii). Combining all the results from the previous two steps, we proof the Theorem.

Proof. The accuracy N is defined as $N = (\mu/\sigma)^2$, and the resolution ν as $\nu = 1/\mu$. We can therefore express

$$N = \left(\frac{\mu}{\sigma}\right)^2 = \frac{1}{\nu^2 \sigma^2}. \quad (\text{A27})$$

From Proposition 7 we know that $\sigma^2 \geq \sigma_\Theta^2$, but $\sigma_\Theta^2 = 1/\Gamma^2$, as we derived in Lemma 2 (see eq. (A12) in the proof). In conclusion,

$$N = \frac{1}{\nu^2 \sigma^2} \leq \frac{1}{\nu^2 \sigma_\Theta^2} = \frac{\Gamma^2}{\nu^2}, \quad (\text{A28})$$

which proves the claim, and thereby the optimality of the family of Heaviside- Θ top-level populations. \square

3. Details on the optimality of the Heaviside population

In Step (ii) of Section A 2, the claim is made that there exists a unique $t_* \geq t_0 = \mu - 1/\Gamma$, such that the two non-tick probabilities coincide $P[t_* \leq T] = e^{-\Gamma(t_* - t_0)}$. To be more precise, we formulate

Proposition 8. *The set $\mathcal{S} = \{t \geq 0 : P[t \leq T] = P_\Theta[t \leq T]\}$ is of the form*

$$\mathcal{S} = [0, a] \sqcup \{t_*\}, \quad (\text{A29})$$

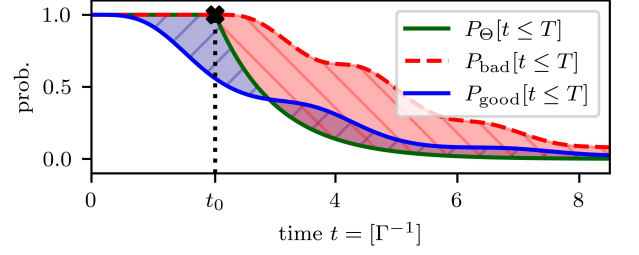


FIG. 7. This sketch visualizes the first step of the the proof of Proposition 8. The solid green line indicates the non-tick probability for the Heaviside population. We see that for the red dashed line which does not fall below 1 before t_0 , the total integral is greater than that of $P_\Theta[t \leq T]$, contradicting the construction, which ensures that both functions have the same integral. The blue, dashed line shows a plausible function for $P[t \leq T]$.

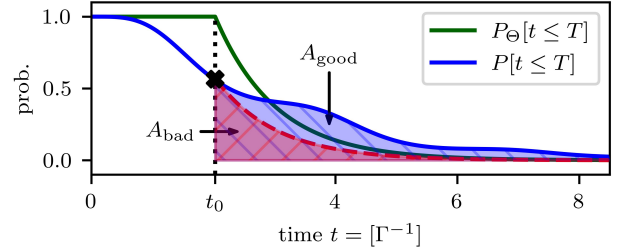


FIG. 8. Here, we visualize step two of the proof of Proposition 8. Again, the solid, green line indicates the non-tick probability for the Heaviside population. To satisfy the construction that $P[t \leq T]$ and $P_\Theta[t \leq T]$ have the same integral on $\mathbb{R}_{\geq 0}$, the area below the graph of $P[t \leq T]$ for $t > t_0$ must be bigger than that of $P_\Theta[t \leq T]$. Thus, at some point after t_0 , $P[t \leq T]$ must be bigger than $P_\Theta[t \leq T]$ (see the blue area denoted by A_{good}), and not always smaller (see red area denoted by A_{bad}).

where $t_* > t_0$, and $[0, a]$ is an interval with upper bound $a < t_0$.

Proof. We divide the proof of this proposition into three steps (a) - (c), with visual aids in Figures 7 and 8.

Step (a). We claim that *there exists a $0 < t < t_0$, such that $P[t \leq T] < 1$* . Suppose that this was not the case, then $P[t \leq T] = 1$ for all $t \leq t_0$ (see Figure 7). By requirement, there must exist a t such that $p(t) \neq p^\Theta(t)$, and because by our (contradictory) assumption t cannot be smaller than t_0 , it must be bigger than t_0 . Since, $P[t \leq T] \geq e^{-\Gamma(t-t_0)}$, for all $t > t_0$, there must exist a $t > t_0$, such that $P[t \leq T] > e^{-\Gamma(t-t_0)}$. But this contradicts the assumption that $\int_0^\infty dt P[t \leq T] = t_0 + 1/\Gamma$. Therefore, it must be that there is a $t < t_0$ with $P[t \leq T] < 1$.

Step (b). Our next claim is, that *there exists an $0 < a < t_0$ such that on $[0, a]$, we have $P[t \leq T] = 1$ and for all other $a < t \leq t_0$, $P[t \leq T] < 1$* . By our previous claim

(1), there exists $0 < t < t_0$ with $P[t \leq T] < 1$. Let a be the infimum of all such t .³ Then, $[0, a] \subset \mathcal{S}$ (continuity of P). Moreover, by the properties of an infimum, for all $\varepsilon > 0$, there exists a $\delta > 0$, such that $P[a + \delta \leq T] < 1$. But $P[t \leq T]$ is monotonically decreasing, hence, this is true for all $\delta > 0$, such that $a + \delta \leq t_0$, proving the claim.

Step (c). In this last step, we show *the existence of a unique $t_* > t_0$ such that $t_* \in \mathcal{S}$* . For a visualization of this step, see Figure 8. The integrals of $P[t \leq T]$ and $P_\Theta[t \leq T]$ on $\mathbb{R}_{\geq 0}$ coincide. However, we have just argued that on a non-empty interval between 0 and t_0 ,

$P[t \leq T]$ is strictly smaller than $P_\Theta[t \leq T]$. This leads to the inequality $\int_0^{t_0} dt P[t \leq T] < \int_0^{t_0} dt P_\Theta[t \leq T]$. In order to ensure that the integrals over all of $\mathbb{R}_{\geq 0}$ are equal, there must exist a $t' > t_0$ such that $P[t' \leq T] > P_\Theta[t' \leq T]$. For all $t > t'$, this inequality must be true too, because $P[t \leq T]$ can not drop faster than $e^{-\Gamma(t-t_0)}$, due to boundedness of the top-level population $p(t) \leq 1$. Set t_* to be the infimum of all such t' . Note that t_* must be strictly greater than t_0 due to continuity of $P[t \leq T]$. This concludes the proof of the last step and therefore of the proposition. \square

³ The set $\{t : P[t \leq T] < 1\}$ is lower bounded by 0 and non-empty by the claim made in step (a), thus, the infimum exists.